0013-7227/91/1296-2845$03.00/0
Endocrinology

Vol. 129, No. 6
Printed in U.S.A.

Multiple Signaling Pathways of V_1-Vascular Vasopressin Receptors of A_7r_5 Cells*

MARC THIBONNIER, ANDREA L. BAYER, MICHAEL S. SIMONSON, AND MARK KESTER

Department of Medicine, University Hospitals of Cleveland and Case Western Reserve University School of Medicine, Cleveland, Ohio 44106-4982

ABSTRACT. We explored the nature and time course of the multiple signal transduction pathways for V_1-vascular vasopressin (AVP) receptors of A_7r_5 aortic smooth muscle cells in culture by using radioligand binding techniques, intracellular calcium monitoring, and polyphosphoinositide and phospholipid analyses.

V_1-vascular AVP receptors of A_7r_5 cells were characterized by the agonist radioligand [^{3}H]AVP and the antagonist radioligand [^{3}H]d(CH_2)$_5$Tyr(Me)AVP. Affinity and capacity of agonist but not antagonist binding were modulated by $MgCl_2$ and aluminum fluoride, suggesting that the receptors are coupled to a guanine nucleotide regulatory protein.

In fura-2-loaded A_7r_5 cells, AVP induced within seconds a dose-dependent increase of free intracellular Ca^{++} ($[Ca^{++}]_i$) consisting of a rapid transient spike and a sustained increase lasting for 3-5 min. The baseline $[Ca^{++}]_i$ was 136 ± 18 nM, the maximum $[Ca^{++}]_i$ response to AVP was 1,582 ± 297 nM, and AVP ED_{50} was 1.87 ± 0.15 nM. Diverse experiments performed with EGTA, 1,2-bis(*O*-aminophenoxy)ethane-*N,N,N',N'*-tetraacetic acid acetoxymethylester, Mn^{++}, ionomycin, terbutylbenzo hydroquinone, and nicardipine suggested that the initial spike resulted from both intracellular Ca^{++} release from the endoplasmic reticulum and extracellular Ca^{++} influx, whereas the sustained phase depended on dihydropyridine-insensitive extracellular Ca^{++} influx. Experiments done with indomethacin and arachidonic acid indicated that AVP-induced extracellular Ca^{++} influx was in part dependent on phospholipase A_2 activation.

In [^{3}H]myoinositol and [^{3}H]arachidonate-labeled A_7r_5 cells, AVP stimulated inositol 1,4,5 trisphosphate and 1,2 diacylglycerol production via activation of phospholipase C. Also, AVP stimulated a transphosphatidylation reaction through activation of phospholipase D in A_7r_5 cells labeled with [^{3}H]1-*O*-alkyl lysoglycerophosphocholine.

Thus, the stimulation of V_1-vascular AVP receptors of A_7r_5 cells triggers several signaling pathways. The immediate and transient $[Ca^{++}]_i$ rise due to mobilization of intracellular and extracellular Ca^{++} is associated with the activation of phospholipases A_2 and C, and the sustained activation of phospholipase D. (*Endocrinology* **129:** 2845-2856, 1991)

VASOPRESSIN (AVP) binds to specific V_1-vascular and V_2-renal membrane receptors which activate distinct second messengers (1). We (2-8) and others (9-11) have described the characteristics of specific V_1-vascular AVP receptors present at the surface of human platelets whose activation leads to calcium mobilization and platelet aggregation. Membrane V_1-vascular AVP receptors also have been characterized in hepatocytes (12), as well as in rat aortic (13) and mesenteric (14) smooth muscle cells.

There is now evidence that many hormones and neurotransmitters act not only through the hydrolysis of phosphatidylinositol 4,5-bisphosphate (PIP_2) to inositol 1,4,5 trisphosphate (Ins[1,4,5]P_3) and 1,2-diacylglycerol (DAG) but also through the breakdown of phosphatidylcholine (PtdCho) (15). The hydrolysis of PtdCho by phospholipase A_2 produces arachidonic acid (AA), whereas hydrolysis of PtdCho by phospholipases C and D leads to the formation of the putative second messengers DAG and phosphatidic acid (PA), respectively. AVP stimulates a PIP_2-specific phospholipase C activity, generating inositol phosphates and DAG, as shown in hepatocytes (15, 16). AVP rapidly but transiently elevates Ins[1,4,5]P_3, whereas DAG production is sustained and remains elevated even at time points where inositol phosphates have returned to basal levels. Sustained DAG production has been linked to phospholipase C-induced hydrolysis of phosphatidylcholine or phosphatidylethanolamine as well as sequential activation of phospholipase D and PA phosphohydrolase. The role of AVP in the temporal production of DAG through such mechanisms needs to be investigated further.

In order to obtain an integrated picture of the interactions of AVP V_1-vascular receptors with a guanine nucleotide regulatory protein, inositol phospholipid metabolism, calcium mobilization, and different phospholi-

Received July 5, 1991.
Address all correspondence and requests for reprints to: Dr. Marc Thibonnier, Division of Endocrinology and Hypertension, Department of Medicine, Case Western Reserve University School of Medicine, 2109 Aldelbert Road, Cleveland, Ohio 44106-4982.
* This work was supported by NIH Grants R01-HL-39757, P01-HL-41618, and R29-AR-40225.

pases activation, we explored the cascade of events from initial binding to several intracellular events triggered by AVP activation of V_1-vascular receptors of A_7r_5 cells. More specifically, we documented: 1) the characteristics of agonist and antagonist binding; 2) the origins of intracellular Ca^{++} ($[Ca^{++}]_i$) mobilized by AVP stimulation; and 3) to what extent AVP-stimulated A_7r_5 cells activate phospholipases A_2, C, and D and generate the putative second messengers arachidonate, diglyceride, and PA, respectively. We also asked whether phosphatidylcholine could serve as a substrate for phospholipases C and D activity.

Materials and Methods

Materials

AVP, Tris-HCl, and other reagents, unless stated otherwise, were from Sigma Chemical Co. (St. Louis, MO). [^{3}H]AVP (SA, 62 Ci/mM) and [^{3}H]d(CH_2)$_5$Tyr(Me)AVP (SA, 56.2 Ci/mM) were from Dupont de Nemours (Wilmington, DE). Ionomycin and 1,2-bis(*O*-aminophenoxy)ethane *N,N,N′,N′*-tetraacetic acid acetoxymethylester (BAPTA) were from Calbiochem Corp. (San Diego, CA). The BCA protein assay reagents were from Pierce Chemical Co. (Rockford, IL). Fura-2 AM was from Molecular Probes Inc. (Eugene, OR). 2,5-Di(tert-butyl)-1,4-benzohydroquinone, (tBuBHQ) was a generous gift from Dr. George Kass, Karolinska Institutet, (Huddinge, Sweden). Cell culture media were from Hazleton Dutchland (Denver, PA). Fetal bovine serum was from Hyclone (Logan, UT). [^{3}H]1-*O*-alkyl lyso glycero-3-phosphocholine (SA, 146 Ci/mM) and [^{3}H] arachidonic acid (SA, 240 Ci/mM) were from Amersham (Arlington Heights, IL). [^{3}H]Myoinositol (SA, 15 Ci/mM) was from ARC (St. Louis, MO). Lipid standards were from Avanti Polar Lipids (Pelham, AL). Silica gel 60 TLC plates (250 μM thickness, heat activated at 110 C) were from EM Science (Gibbstown, NJ).

Culture of A_7r_5 vascular smooth muscle cells

A_7r_5 cells are an established smooth muscle cell line derived from rat embryo aorta (17) in which AVP stimulates inositol phosphate production, calcium mobilization, and electrical activity of ionic channels (18, 19). The A_7r_5 cells were obtained from the American Tissue Culture Collection (Rockville, MD). The cells were grown at 37 C in Dulbecco's modified Eagle's medium (DMEM) supplemented with 10% fetal calf serum and antibiotics (100 U/ml penicillin and 100 μg/ml streptomycin) under a 5% CO_2 atmosphere. A_7r_5 cells were subcultured every 7 days in 100-mm Petri dishes using 0.05% trypsin-0.02% EDTA, whereas media were renewed every 2–3 days.

Preparation of membranes from cultured A_7r_5 cells

Three days after trypsinization, subconfluent monolayers of A_7r_5 cells were washed twice with physiological saline solution (PSS containing in mM: 140 NaCl, 4.6 KCl, 10 glucose, 10 HEPES, pH 7.4) before dispersion with a cell scraper in 10 ml PSS. After rinsing with 10 ml PSS, the cells were concentrated by centrifugation at 2,000 × *g* for 5 min at 4 C and resuspended in 5 ml hypotonic buffer (5 mM Tris-HCl, 5 mM EDTA, pH 7.4) for homogenization by 10 strokes with a glass-Teflon pestle. The membrane preparations were washed twice by centrifugation at 50,000 × *g* for 15 min at 4 C and resuspended in buffer 50 mM Tris-HCl, 20% glycerol for storage at −70 C.

Radioligand binding experiments

Saturation experiments of AVP receptors of membrane preparations of A_7r_5 cells were performed at 30 C in buffer 50 mM Tris-HCl, 20% glycerol, pH 7.4, supplemented with increasing concentrations of [^{3}H]AVP (±2.5 μM unlabeled AVP) and 10 mM $MgCl_2$ or [^{3}H]d(CH_2)$_5$Tyr(Me)AVP [±1 μM unlabeled d(CH_2)$_5$Tyr(Me)AVP] in duplicate tubes. After 30 min incubation, filtration was achieved through GF/B glass fiber filters soaked in 1% polyethyleneimine (2–6) and set on a Brandel filtration unit (Brandel, Gaithersburg, MD). The radioactivity retained on the filters was measured by liquid scintillation spectrometry (Beckman counter LS 5801, Beckman Instruments, Palo Alto, CA; yield = 64%). Affinity (K_d) and capacity (B_{max}) of the AVP receptors were calculated by a nonlinear least square analysis program (2). Protein concentration was measured with Pierce's BCA reagent using ovalbumin as an internal standard. Competition experiments were also performed at 30 C for 30 min with membrane preparations of A_7r_5 cells, one concentration of [^{3}H]AVP (3–5 nM), and increasing concentrations of AVP V_1-vascular and V_2-renal agonists. IC_{50} values for competitors' inhibition of [^{3}H]AVP binding were determined from dose-response curves and converted into inhibition constant (K_i) values according to the equation of Cheng and Prusoff (20).

Measurements of intracellular calcium

Serum-starved monolayer cultures of A_7r_5 cells were grown on ACLAR plastic coverslips (14 × 14 mm, Allied Engineered Plastics, Pottsville, PA) as previously described (21) and were assayed 2 days later. Cell monolayers (1–2 × 10^5 cells/cm^2) were loaded in serum-free DMEM with fura-2 AM (1 μM/coverslip) for 40 min at 37 C. The permeable acetoxymethyl ester of fura-2 is hydrolyzed by cellular esterases upon entering the cells, and the fura-2 formed is relatively impermeable and becomes trapped inside the cells. The monolayers of A_7r_5 cells were washed, then transferred to serum-free, fura-2-free medium and incubated an additional 20 min at 37 C. The loaded monolayers were stored on ice in buffer Krebs-Henseleit-HEPES (KHH, containing in mM: 130 NaCl, 5 KCl, 1.25 $CaCl_2$, 0.8 $MgSO_4$, 5.5 glucose, 20 HEPES, and 0.1% fatty acid free BSA, pH 7.4) until used. The coverslips were placed into a quartz cuvette containing 2 ml KHH buffer and maintained at 37 C with continuous stirring. When thermal equilibrium was reached, the fluorescence signal was recorded with a Case Western Reserve University spectrofluorometer [340 nm excitation and 500 nm emission wavelengths as previously reported, (22)]. After recording the baseline signal for 5 min, increasing concentrations of AVP were added to the cuvette to stimulate the mobilization of intracellular calcium and the influx of extracellular calcium. Fluorescence measurements were converted to intracellular calcium concentrations $[Ca^{++}]_i$ by determining maximal fluorescence (F_{max}) with the nonfluorescent Ca^{++} ionophore, ionomycin (25 μM), followed by minimal flu-

orescence (F_{min}) obtained by addition of 1.25 mM $MnCl_2$. The following formula was then used: $[Ca^{++}]_i = K_d \times (F - F_{min})/(F_{max} - F)$, with K_d for fura-2 = 224 nM. Autofluorescence by the cells or agonists as well as fura-2 leak outside the cells was negligible. In experiments where BAPTA was used, 10 μM BAPTA acetoxymethylester was added and coincubated with fura-2 in DMEM as described above.

Measurement of polyphosphoinositide formation

The measurement of water-soluble inositol phosphates (IPn) was performed as previously described using anion-exchange chromatography (23). Authentic [^{3}H]inositol[1]-phosphate (IP_1), [^{3}H]inositol[1,4]-bisphosphate (IP_2), and [^{3}H]inositol[1,4,5]-trisphosphate (IP_3) were used to standardize the Dowex resin columns and establish recoveries.

Radiolabeling and extraction of membrane phospholipids

As described previously for HL60 cells and mesangial cells (23, 24), A_7r_5 cells were grown in either 60-mm Petri dishes and labeled for 2 h with 1 μCi/ml [^{3}H]1-*O*-alkyl lyso glycero-3-phosphocholine ([^{3}H]-alkyl lyso GPC) in calcium-free KHH buffer for measurement of PA and phosphatidylethanol (PtdEt) or in 12-well cluster dishes and labeled for 3 h with 1 μCi/ml [^{3}H]arachidonate in complete KHH buffer for DAG measurements. The radioisotopes were removed by extensive washing on ice, and the cells were warmed at 37 C in complete KHH buffer. One micromolar AVP in 0.2% BSA was added for variable times. For PA and PtdEt experiments, AVP was added in the presence or absence of 0.5% ethanol. The incubation was terminated 15 min later with ice-cold acidified methanol, and the cells were scraped and transferred into an equal vol of chloroform. The cultures were scraped again in methanol to yield a chloroform/methanol/water ratio of 1/2/0.8. After 45 min at 4 C, the methanol and chloroform extracts were adjusted to yield two phases (chloroform/methanol/water, 1/1/0.9 vol/vol/vol). The chloroform lipid extracts were separated, and the methanol/water extracts were rewashed with chloroform. The combined chloroform extracts were dried under nitrogen and resuspended in 100 μl 90% chloroform/10% methanol. The samples were spiked with authentic synthetic PA and PtdEt or 1,2-diolein, then spotted on silica gel 60 TLC plates. For the PA/PtdEt experiments, phospholipids were eluted from the origin with a mobile phase consisting of chloroform/methanol/acetic acid, 65/15/6, vol/vol/vol, and for the DAG experiments, neutral lipids were separated by a benzene/diethyl ether/ammonia, 100/80/0.2, vol/vol/vol solvent system. With the above elution systems, PtdEt was well resolved from several phospholipid contaminants including bis-phosphatidic acid, cardiolipin, and phosphatidyl glycerol. Also, the DAG solvent system separated 1,2 DAG from 1,3 DAG, triacylglycerol, monoacylglycerol, and free fatty acids. The lipids were visualized by toluidino-2-naphthalene sulfonic acid spray and UV light. The radiolabeled lipids which comigrate with the internal standards were scraped and radioactivity determined in a liquid scintillation counter.

Presentation of data

Each set of experiments was performed at least on three different occasions, and each individual experiment was run in triplicate. Results in the text and tables are expressed as mean ± SEM. Statistical analysis used nonparametric tests including Wilcoxon signed-rank test and Friedman two-way analysis of variance (Statview statistical package for the Macintosh computer). *P* values less than 0.05 were considered as statistically significant.

Results

Identification and characterization of specific AVP receptors of A_7r_5 cells

Kinetics of [^{3}H]AVP binding to plasma membranes of A_7r_5 cells. The amount of [^{3}H]AVP specific binding to A_7r_5 plasma membranes is protein concentration dependent (Fig. 1A). Within a protein concentration range from 0.10–0.60 mg/ml, a linear increase in [^{3}H]AVP specific binding was observed (r = 0.99, eight different protein concentrations, n = 3). Specific binding accounted for 58 ± 3% of total binding at the [^{3}H]AVP concentration used (4.85 ± 0.30 nM). [^{3}H]AVP specific binding to plasma membranes of A_7r_5 cells is time dependent and reached an equilibrium value of 78 ± 2% of total binding within 30 min of incubation at 30 C with 3.81 ± 0.20 nM [^{3}H]AVP (protein concentration = 0.61 ± 0.20 mg/ml, n = 3, Fig. 1B). The association kinetics could be fitted best by the following equation, $B = B_{eq}(1 - \exp^{-K_1 * t})$ where B is specific binding at a given time and B_{eq} is specific binding reached at equilibrium (B_{eq} = 1906 cpm, K_1 = 0.127 min^{-1}, r = 0.996). [^{3}H]AVP specific binding to plasma membranes of A_7r_5 cells was rapidly reversible, as shown on Fig. 1C. To demonstrate reversibility, plasma membranes of A_7r_5 cells (protein concentration = 0.32 ± 0.10 mg/ml) were incubated with 3.86 ± 0.23 nM [^{3}H]AVP for 30 min; thereafter, a high concentration of unlabeled AVP (1 μM) was added to the incubation mixture, and remaining [^{3}H]AVP specific binding was measured at serial time intervals after addition of unlabeled AVP. Unlabeled AVP rapidly displaced [^{3}H]AVP from the binding sites. Forty-five minutes after addition of unlabeled AVP, no specific binding of [^{3}H]AVP was left. The dissociation kinetic could be fitted best by the following equation, $B = B_{eq}(\exp^{-K_2 * t})$ where B is specific binding at a given time after addition of unlabeled AVP and B_{eq} is equilibrium specific binding reached before addition of unlabeled AVP (B_{eq} = 1006 cpm, K_2 = 0.167 min^{-1}, r = 0.996). Thus, the equilibrium dissociation constant, K_d, for [^{3}H]AVP binding determined from association and dissociation experiments was 1.31 nM.

Concentration of A_7r_5 cells [^{3}H]AVP binding sites. Saturation equilibrium binding experiments were performed with membrane preparations of A_7r_5 cells (protein concentration = 0.25 ± 0.06 mg/ml), and eight different concentrations (0.40–16 nM) of the agonist radioligand [^{3}H]AVP in the presence or absence of 2.5 μM unlabeled

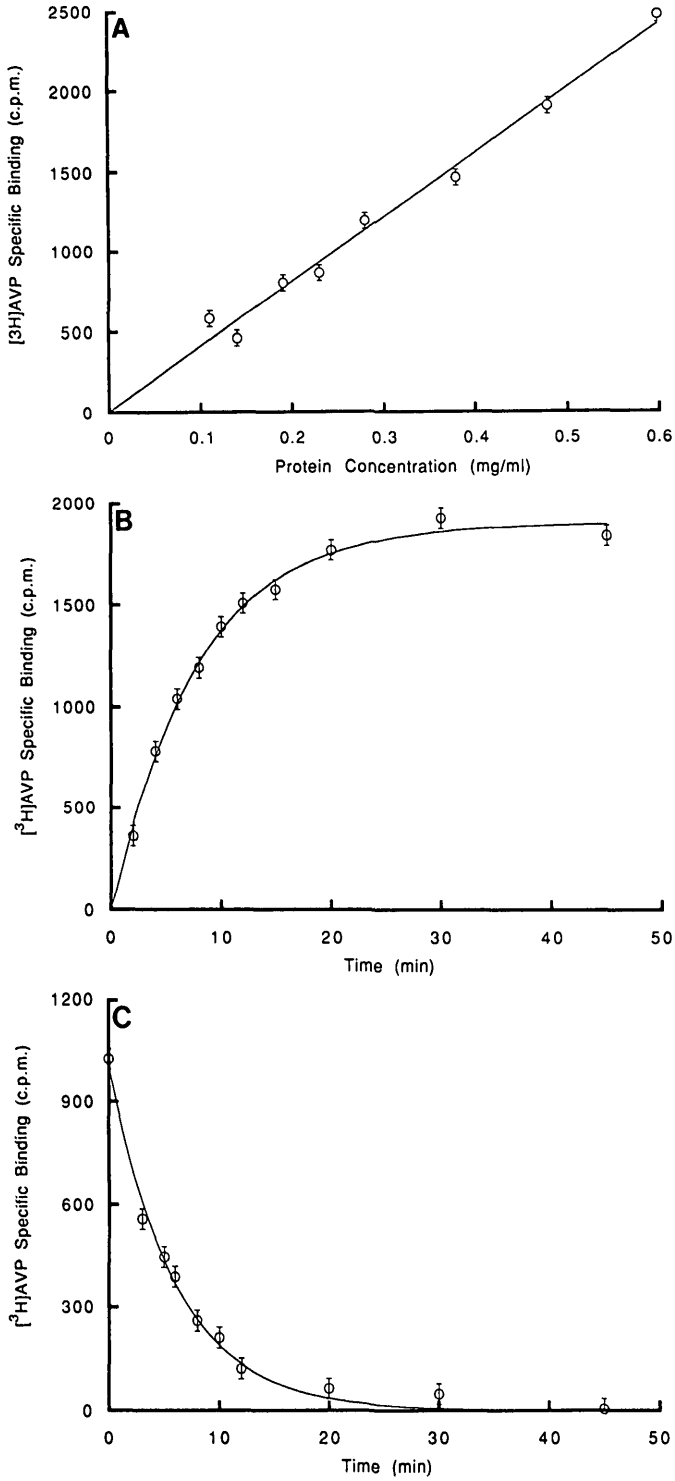

FIG. 1. A, [^{3}H]AVP specific binding to A_7r_5 cell plasma membranes as a function of protein concentration. B, [^{3}H]AVP specific binding to A_7r_5 cell plasma membranes as a function of time. C, Reversibility of [^{3}H]AVP specific binding to A_7r_5 cell plasma membranes.

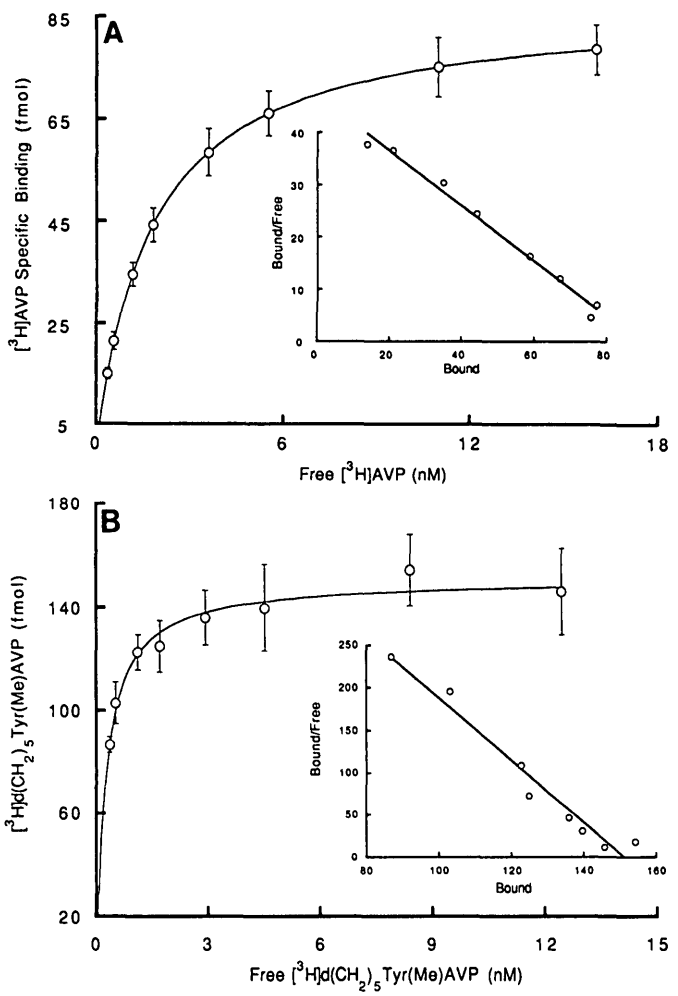

FIG. 2. A, Saturation equilibrium specific binding of [^{3}H]AVP to A_7r_5 cell plasma membranes. *Inset,* Scatchard linear transformation of the data. B, Saturation equilibrium specific binding of [^{3}H] $d(CH_2)_5Tyr(Me)AVP$ to A_7r_5 cell plasma membranes. *Inset,* Scatchard linear transformation of the data.

AVP. As shown on Fig. 2A, analysis of [^{3}H]AVP specific binding to V_1-vascular receptors of A_7r_5 cells showed that data could be fitted best by the following equation $B = (B_{max}{}^*L_f)/(L_f + K_d)$ where B = concentration of bound tracer, B_{max} = total concentration of receptors, L_f = concentration of unbound tracer, K_d = dissociation constant of the receptor. One single class of receptors was identified with a K_d of 2.11 ± 0.11 nM and a B_{max} of 306 ± 10 fmol/mg protein (n = 11). Total binding represented 4 ± 0.2% to 1.3 ± 0.01% of total ligand concentration when the tracer concentration was increased from 0.40 ± 0.02 to 16 ± 1.2 nM. Nonspecific binding increased linearly from 25 ± 3% to 70 ± 4% when ligand concentration was raised from 0.40 ± 0.02 to 16 ± 1.2 nM (r = 0.998).

Demonstration of the V_1-vascular nature of AVP receptors of A_7r_5 cells

Saturation equilibrium binding experiments were also performed with membrane preparations of A_7r_5 cells (protein concentration = 0.35 ± 0.05 mg/ml) and the V_1-vascular antagonist [^{3}H]$d(CH_2)_5Tyr(Me)AVP$ (eight different concentrations from 0.4–12 nM) in the presence

or absence of 1 μM unlabeled $d(CH_2)_5Tyr(Me)AVP$. One single class of binding sites was identified with a K_d of 0.31 ± 0.05 nM and a B_{max} of 420 ± 13 fmol/mg protein (n = 10, Fig. 2B). Thus, the excellent affinity of the V_1-vascular antagonist for the AVP receptors of A_7r_5 cells supports their belonging to the V_1-vascular subtype.

Competitive inhibition of [^{3}H]AVP agonist binding to V_1-vascular AVP receptors of A_7r_5 cells by various AVP V_1 and V_2 analogs were carried out to confirm the V_1-vascular subtype of the A_7r_5 AVP receptors. In competition experiments, A_7r_5 cell membranes were incubated at 30 C with one fixed concentration of [^{3}H]AVP (3–5 nM) and increasing concentrations of AVP analogs. Analysis of the agonists' competition for [^{3}H]AVP binding was fitted best by one single site model. Displacement of [^{3}H]AVP by unlabeled AVP confirmed the presence of one single class of binding sites (K_i = 1.53 ± 0.32 nM, n = 3). The dissociation constants (K_i) of the different AVP analogs are shown in Table 1. As indicated in Fig. 3, there was a significant correlation between the binding dissociation constant values of these agonists and their corresponding vasopressor activities ($r = 0.91$, $P < 0.001$), whereas there was no correlation between the same binding dissociation constant and their antidiuretic potency ($r = 0.15$). These findings therefore confirm that AVP receptors of A_7r_5 cells belong to the V_1-vascular subtype.

Interaction of V_1-vascular AVP receptors of A_7r_5 cells with a GTP binding protein

Several lines of experiments were performed to demonstrate a link between V_1-vascular AVP receptors of A_7r_5 cells and a guanine nucleotide regulatory protein. The influence of the mixture of 10 mM sodium fluoride/10 μM aluminum chloride (which mimics the effects of GTP on agonist binding) on the affinity and capacity of AVP receptors of A_7r_5 cells was tested in saturation equilibrium binding experiments with membrane preparations of A_7r_5 cells and the agonist radioligand [^{3}H]AVP in the presence or absence of $MgCl_2$. As shown in Table 2, the affinity of A_7r_5 cells V_1-vascular receptors for [^{3}H]AVP was low in the absence of $MgCl_2$ and was reduced even further by addition of aluminum fluoride. The addition of $MgCl_2$ improved the affinity of the receptors for [^{3}H]AVP. In the presence of $MgCl_2$, the addition of aluminium fluoride slightly modified the affinity of the receptors for [^{3}H]AVP. The total number of binding sites available to [^{3}H]AVP was not influenced by aluminum

TABLE 1. Affinity constants for binding of AVP and agonists to plasma membranes of A_7r_5 cells: relation to vasopressor and antidiuretic activities

Compound	pK_i	Vasopressor activity (U/mg)	Antidiuretic activity (U/mg)
AVP	8.82	382	323
Phe2Om8OT	8.38	124	0.55
dAVP	8.20	346	1745
AVT	8.13	196	274
LVP	6.99	229	258
dDAVP	5.69	0.39	1200
OXY	6.44	4	4.3
8DAVP	5.40	1.1	257

Competition experiments were performed for 30 min at 30 C with A_7r_5 cell membrane preparations, 3–5 nM [^{3}H]AVP and increasing concentrations of AVP V_1 vascular and V_2-renal agonists (n = 3 for each analog). $pK_i = -\log K_i$, K_i = binding dissociation constant at equilibrium for the corresponding analog (M). Vasopressor and antidiuretic activities come from Ref. 41. AVP, [8-arginine]vasopressin; Phe2Orn8OT, [2-phenylalanine, 8-ornithine]oxytocin; LVP, [8-lysine]vasopressin; OXY, oxytocin; AVT, arginine-vasotocin; dAVP, [1-deamino, 8-arginine]vasopressin; 8DAVP, [8-D-arginine]vasopressin; dDAVP, [1-deamino, 8-D-arginine]vasopressin.

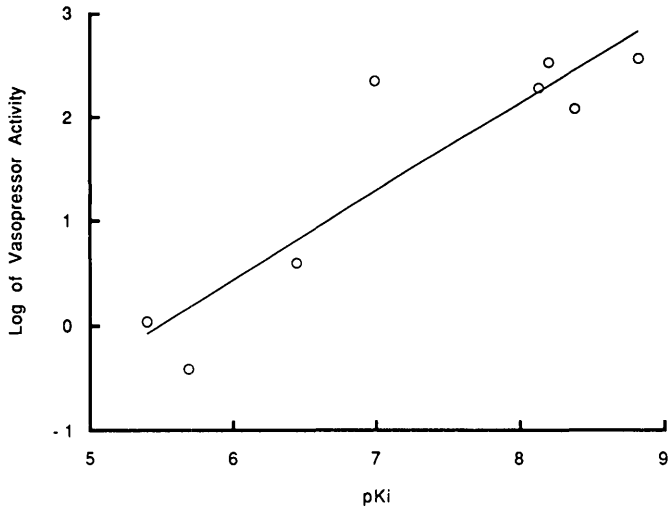

FIG. 3. Relationship between AVP agonists' binding to A_7r_5 cell plasma membranes and their vasopressor activities *in vivo*. The graph was constructed by using data given in Table 1. $pK_i = -\log K_i$, K_i = binding dissociation constant at equilibrium for the corresponding analog (M). Vasopressor activities come from reference 41.

TABLE 2. Effects of $MgCl_2$ and aluminum fluoride (AlF) on agonist and antagonist binding to AVP receptors of A_7r_5 cells

	[^{3}H]AVP		[^{3}H] $d(CH_2)_5Tyr(Me)AVP$	
	K_d (nM)	B_{max} (fmol/mg)	K_d (nM)	B_{max} (fmol/mg)
Control	7.77 ± 0.79[a]	243 ± 11[a]	0.31 ± 0.05	420 ± 13
+AlF	53.28 ± 3.45[a]	256 ± 23[a]	0.16 ± 0.05	439 ± 25
+$MgCl_2$	2.11 ± 0.11	306 ± 10	0.60 ± 0.06	407 ± 23
+$MgCl_2$ and AlF	2.63 ± 0.21	310 ± 15	0.57 ± 0.04	411 ± 20

Saturation experiments were performed with A_7r_5 cell membrane preparations and increasing concentrations of [^{3}H]AVP or [^{3}H] $d(CH_2)_5Tyr(Me)AVP$ for 30 min at 30 C in the absence or presence of $MgCl_2$ alone or with AlF (n = 3 for each series). K_d, binding equilibrium dissociation constant; B_{max}, maximum number of binding sites.

[a] $P < 0.05$ compared to the series incubated in the presence of $MgCl_2$.

fluoride. Saturation equilibrium binding experiments were also performed with membrane preparations of A_7r_5 cells and the V_1-vascular antagonist radioligand [^{3}H] $d(CH_2)_5Tyr(Me)AVP$. In the absence of $MgCl_2$, the affinity of the receptors for [^{3}H]$d(CH_2)_5Tyr(Me)AVP$ was already high and was not altered by addition of aluminium fluoride (Table 2). Addition of $MgCl_2$ alone or in association with aluminium fluoride did not modify significantly the high affinity of the receptors for the V_1-vascular antagonist. The total number of binding sites available to [^{3}H]$d(CH_2)_5Tyr(Me)AVP$ was independent of $MgCl_2$ and aluminum fluoride.

Intracellular calcium increase by activation of V_1-vascular AVP receptors of A_7r_5 cells

An increase of $[Ca^{++}]_i$, the hallmark of V_1-vascular AVP receptor activation, was measured in fura-2 loaded A_7r_5 cells. The basal $[Ca^{++}]_i$ in fura-2-loaded A_7r_5 cells was 136 ± 18 nM (n = 34). Stimulation of A_7r_5 cells by AVP resulted in a biphasic increase in $[Ca^{++}]_i$ composed of a rapid (within 2–5 sec) and transient spike, followed by a smaller increase with return to basal levels 3–5 min after addition of AVP (Fig. 4A). Preaddition of an equimolar dose of the V_1-vascular antagonist $d(CH_2)_5Tyr(Me)AVP$ blocked AVP-induced increase of $[Ca^{++}]_i$, but did not interfere with ionomycin mobilization of Ca^{++}, confirming the V_1-vascular nature of the AVP receptors involved (Fig. 4B). An initial stimulation with 1 μM AVP was followed by a dramatic reduction of $[Ca^{++}]_i$ response to a subsequent identical challenge with AVP, suggesting down-regulation and/or desensitization of the receptors (Fig. 4C). The $[Ca^{++}]_i$ response to AVP was concentration dependent as shown on Fig. 4D, with an ED_{50} = 1.87 ± 0.15 nM AVP (n = 3) calculated from the equation $E = (E_{max}*C)/(ED_{50} + C)$ where E = response to AVP, E_{max} = maximum response induced by AVP, ED_{50} = concentration of AVP inducing half-maximum response, and C = concentration of AVP (25). The maximal $[Ca^{++}]_i$ response induced by 1 μM AVP was 1582 ± 297 nM (n = 15).

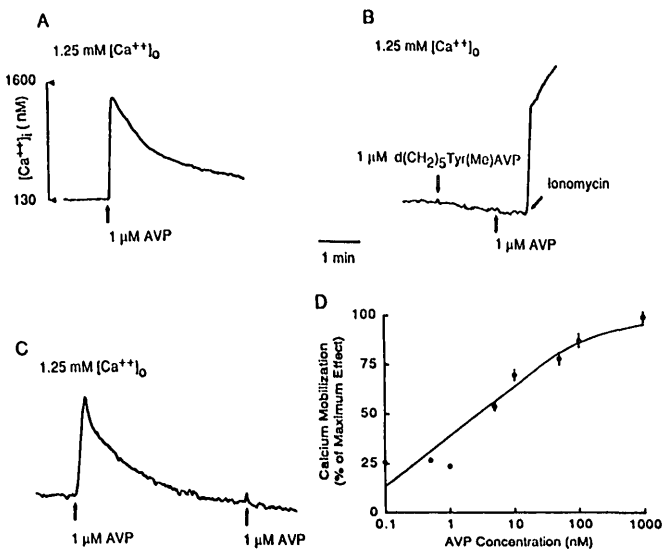

FIG. 4. $[Ca^{++}]_i$ waveforms induced by AVP in A_7r_5 cells. A_7r_5 cell monolayers on ACLAR coverslips were loaded with fura-2 and incubated in KHH buffer, pH 7.4. Basal $[Ca^{++}]_i$ was measured fluorometrically after reaching thermal equilibrium at 37 C. A, One micromolar AVP was added in the presence of extracellular Ca^{++}; B, 1 μM V_1-vascular antagonist $d(CH_2)_5Tyr(Me)AVP$ followed by 1 μM AVP were added in the presence of extracellular Ca^{++}; C, Two doses of 1 μM AVP were added at 3-min intervals in the presence of extracellular Ca^{++}; D, relationship between AVP dose and $[Ca^{++}]_i$ waveform amplitude in A_7r_5 cells.

Source of $[Ca^{++}]_i$ increase induced by activation of V_1-vascular AVP receptors of A_7r_5 cells

The increase in $[Ca^{++}]_i$ induced by AVP could result from the release of intracellular stores, the influx of Ca^{++}, the reduction of Ca^{++} efflux, or a combination of these mechanisms. When AVP was added in the absence of extracellular Ca^{++}, the transient increase in $[Ca^{++}]_i$ was blunted and the sustained phase was abolished (Fig. 5A). A similar profile was noted when AVP was added after application of 4 mM EGTA (Fig. 5B). The maximal

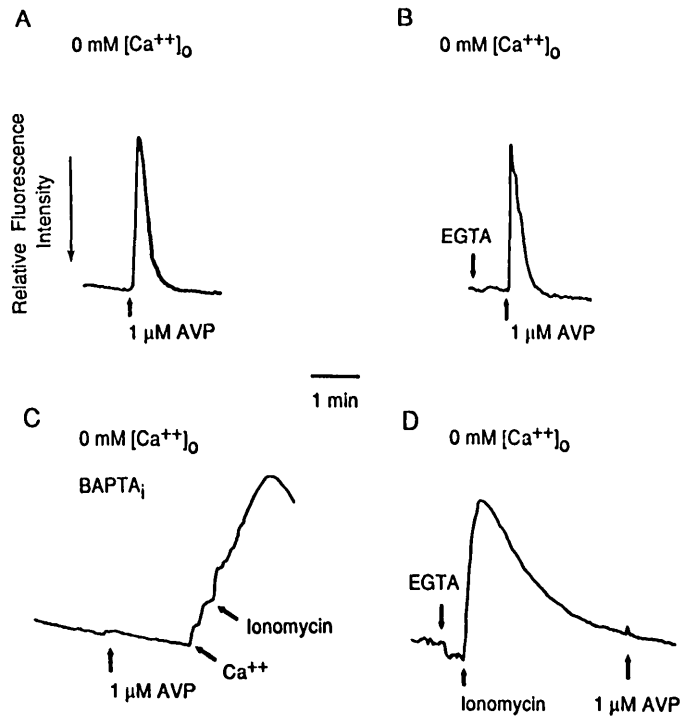

FIG. 5. Relative contribution of the mobilization of intracellular Ca^{++} stores and of the influx of extracellular Ca^{++} to the $[Ca^{++}]_i$ waveforms induced by AVP in A_7r_5 cells. A, One micromolar AVP was added in the absence of extracellular Ca^{++}. B, A_7r_5 cells incubated in the absence of extracellular Ca^{++} were treated with 4 mM EGTA for 30 sec before addition of 1 μM AVP. C, A_7r_5 cells were coloaded with fura-2 and BAPTA and resuspended in the absence of extracellular Ca^{++} before addition of 1 μM AVP then extracellular Ca^{++} and ionomycin. D, A_7r_5 cells were loaded with fura-2 and resuspended in the absence of extracellular Ca^{++} before addition of EGTA, then ionomycin and AVP.

$[Ca^{++}]_i$ response induced by 1 μM AVP in the absence of extracellular Ca^{++} was 788 ± 186 nM (n = 10). These experiments suggest that the initial $[Ca^{++}]_i$ peak is mostly due to mobilization of intracellular calcium, whereas the persistant elevation of $[Ca^{++}]_i$ abolished by extracellular Ca^{++} depletion and EGTA is related to the influx of extracellular Ca^{++}. To confirm the intracellular origin of the initial $[Ca^{++}]_i$ spike induced by AVP, A_7r_5 cells were loaded with 10 μM BAPTA, a high affinity Ca^{++} chelator which does not interfere with the fluorescence determination of $[Ca^{++}]_i$ with fura-2. AVP (1 μM) failed to elevate $[Ca^{++}]_i$ when added to A_7r_5 cells loaded with both fura-2 and BAPTA and incubated in Ca^{++}-free medium (Fig. 5C). Subsequent addition of extracellular Ca^{++} and ionomycin confirmed that BAPTA loading did not interfere with the fura-2 detection system (Fig. 5C). Further evidence that AVP releases Ca^{++} from an intracellular pool was obtained by depletion of intracellular stores with ionomycin and EGTA before addition of AVP. As shown on Fig. 5D, depletion of the intracellular Ca^{++} stores prevented any increase in $[Ca^{++}]_i$ in response to AVP. Taken together, the experiments presented in Figs. 4 and 5 suggest that the initial spike in $[Ca^{++}]_i$ results from both intracellular release of Ca^{++} and extracellular influx of Ca^{++}, whereas the sustained phase of $[Ca^{++}]_i$ depends on extracellular calcium influx.

Mobilization of Ca^{++} from the endoplasmic reticulum pool by activation of V_1-vascular AVP receptors of A_7r_5 cells

To further analyze the intracellular pool of Ca^{++} released by AVP, we used tBuBHQ, a relatively selective inhibitor of endoplasmic reticulum Ca^{++}-ATPase, which prevents uptake of Ca^{++} into the pool released by inositol[1,4,5]P_3 (26). In the absence of extracellular Ca^{++}, tBuBHQ (25 μM) caused a rapid increase in Ca^{++}, presumably by depletion of the intracellular stores followed by a progressive decline linked to Ca^{++} efflux (Fig. 6A). The subsequent addition of ionomycin provoked the reentry of Ca^{++}, indicating that tBuBHQ did not interfere with the Ca^{++}/fura-2 detection system. In the presence of extracellular Ca^{++}, the same pattern was observed but with a greater influx of Ca^{++} after administration of ionomycin (Fig. 6B). The response to the addition of AVP after tBuBHQ under conditions in which Ca^{++} stores can no longer be replenished by extracellular Ca^{++} influx was massively reduced, suggesting that AVP and tBuBHQ act on the same intracellular pool of Ca^{++} (Fig. 6C). These experiments with tBuBHQ suggest that AVP releases Ca^{++} from the endoplasmic reticulum pool, presumably the same pool sensitive to Ins[1,4,5]P_3 (27).

Gating of a plasma membrane Ca^{++} channel by activation of V_1-vascular AVP receptors of A_7r_5 cells

Further evidence that AVP increases transmembrane divalent cation permeability was obtained by using

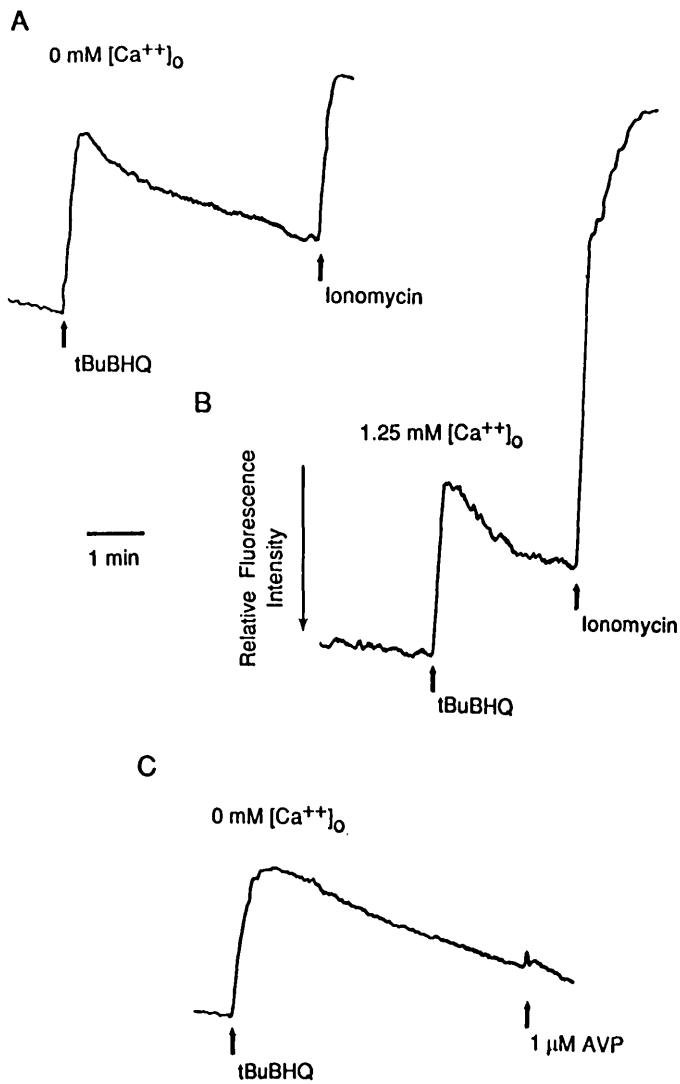

FIG. 6. AVP mobilization of Ca^{++} from the endoplasmic reticulum pool of A_7r_5 cells. tBuBHQ was added to fura-2-loaded A_7r_5 cells in the absence (A) or presence (B) of extracellular calcium. tBuBHQ then AVP were added in the absence of extracellular calcium (C).

Mn^{++}, a divalent cation which permeates Ca^{++} channels in other cells (26). Mn^{++} binds with high affinity to fura-2, but unlike Ca^{++}, Mn^{++} quenches fura-2 fluorescence. When 10 μM Mn^{++} was added to fura-2-loaded A_7r_5 cells in Ca^{++}-free medium, the fluorescence intensity declined gradually, in relation with continuous influx of Mn^{++} (Fig. 7A). Addition of ionomycin, which facilitates Mn^{++} translocation, provoked a dramatic potentiation of fura-2 quenching. Chelation of extracellular Mn^{++} with excess EGTA prevented the further decline in fluorescence but failed to reverse this decline, suggesting that Mn^{++} efflux from the cells was negligible (Fig. 7B). Therefore, in A_7r_5 cells measuring the rate of fura-2 quenching by exogenous addition of Mn^{++} can measure unidirectional divalent cation uptake. When Mn^{++} was added immediately before the addition of 1 μM AVP, the transient increase

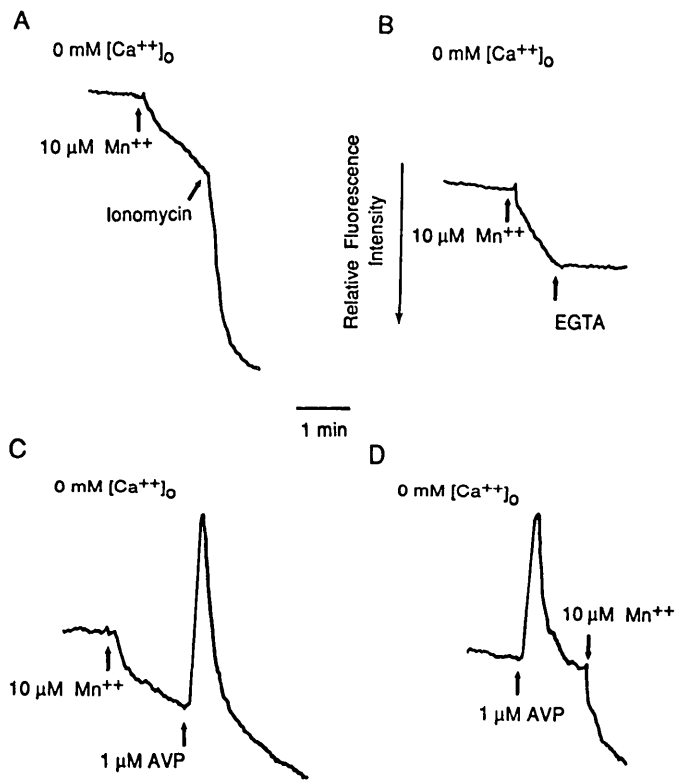

FIG. 7. AVP gating of a plasma membrane Ca^{++} channel of A_7r_5 cells. Fura-2-loaded A_7r_5 cells were suspended in calcium-free medium then challenged with Mn^{++} followed by ionomycin (A) or EDTA (B). Mn^{++} was added before (C) or after AVP (D).

in fura-2 fluorescence was blunted and marked quenching of fura-2 fluorescence occurred within seconds after AVP addition (Fig. 7C). When Mn^{++} was added 1 min after AVP, fura-2 fluorescence was also rapidly quenched (Fig. 7D). These results suggest that AVP increases within seconds the influx of divalent cations.

V_1-vascular AVP receptors of A_7r_5 cells stimulate influx of extracellular Ca^{++} via a dihydropyridine-insensitive Ca^{++} channel

The sustained, extracellular Ca^{++}-dependent phase of $[Ca^{++}]_i$ increase can be explained by the activation of receptor-gated Ca^{++} channels or of voltage-gated Ca^{++} channels. Pretreatment with 10 μM nicardipine failed to change either the transient or the sustained phase of $[Ca^{++}]_i$ induced by AVP, suggesting that AVP-induced $[Ca^{++}]_i$ influx occurs via a dihydropyridine-insensitive Ca^{++} channel, most likely through activation of a receptor-gated Ca^{++} channel (Fig. 8A). In the absence of extracellular Ca^{++}, AVP causes only a transient and smaller increase in $[Ca^{++}]_i$, but the rapid increase in $[Ca^{++}]_i$ after repletion of extracellular Ca^{++} suggests that the channels activated by AVP remain open (Fig. 8B). Clamping of intracellular Ca^{++} with BAPTA prevents the transient increase in $[Ca^{++}]_i$ by AVP, but extracellular Ca^{++} repletion still increases $[Ca^{++}]_i$ (Fig. 8C).

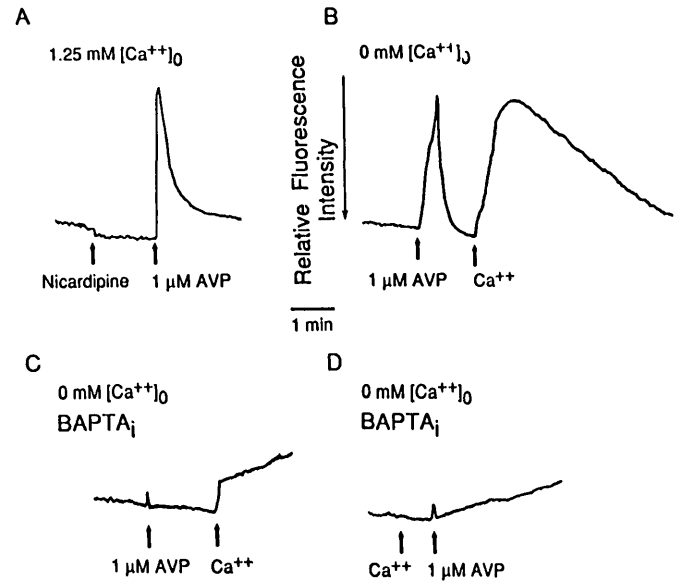

FIG. 8. AVP-stimulated influx of Ca^{++} is dihydropyridine insensitive. Fura-2-loaded A_7r_5 cells were stimulated by AVP in the presence of calcium and nicardipine (A). In calcium-free medium, AVP then Ca^{++} were subsequently added (B). AVP and calcium were added in alternate order in cells depleted of extra and intracellular calcium (C and D).

Gating of AVP-sensitive Ca^{++} channels was independent of intracellular Ca^{++} as shown in BAPTA-clamped A_7r_5 cells when extracellular Ca^{++} was added before AVP (Fig. 8D).

V_1-vascular AVP receptors of A_7r_5 cells stimulate influx of extracellular Ca^{++} via a phospholipase A_2 sensitive mechanism

In the presence of extracellular Ca^{++}, pretreatment of A_7r_5 cells with 20 μM indomethacin reduced the height of the initial $[Ca^{++}]_i$ transient and shortened the sustained $[Ca^{++}]_i$ increase induced by AVP (Fig. 9, A and B). In calcium-free medium, indomethacin preaddition did not significantly alter the shape of the $[Ca^{++}]_i$ transient (data not shown). These results suggest that AVP-induced extracellular Ca^{++} influx involves an arachidonate-derived second messenger and presumably phospholipase A_2 activation. This hypothesis is further supported by the fact that in the presence of extracellular Ca^{++}, addition of 10 μM AA induced an increase in $[Ca^{++}]_i$ (Fig. 9C). The subsequent response to AVP was of short duration, suggesting that the AA-sensitive influx pathway desensitizes, thus preventing subsequent activation by AVP.

AVP stimulates the formation of inositol phosphates in A_7r_5 cells

AVP stimulated the accumulation of the various polyphosphoinositides in a time-dependent manner (Fig. 10A). Ins[1]P production was stimulated only after 1 min and was increased by 181% at 5 min (12,563 ± 2,532 cpm

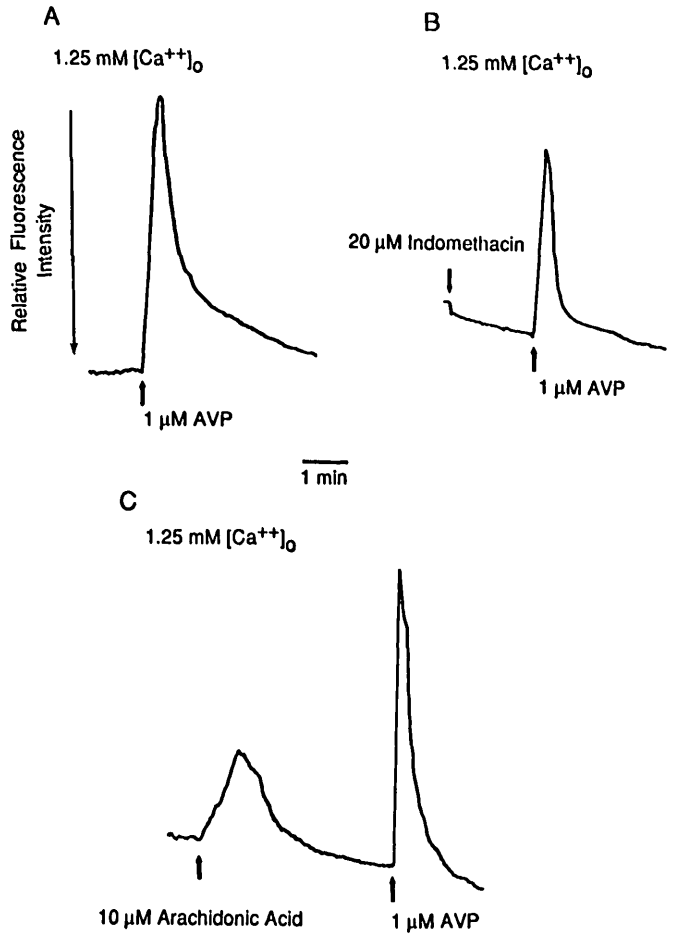

FIG. 9. AVP-stimulated influx of Ca^{++} activates phospholipase A_2. In the presence of extracellular calcium, fura-2-loaded A_7r_5 cells were stimulated by AVP in the absence (A) or the presence (B) of indomethacin or in the presence of AA (C).

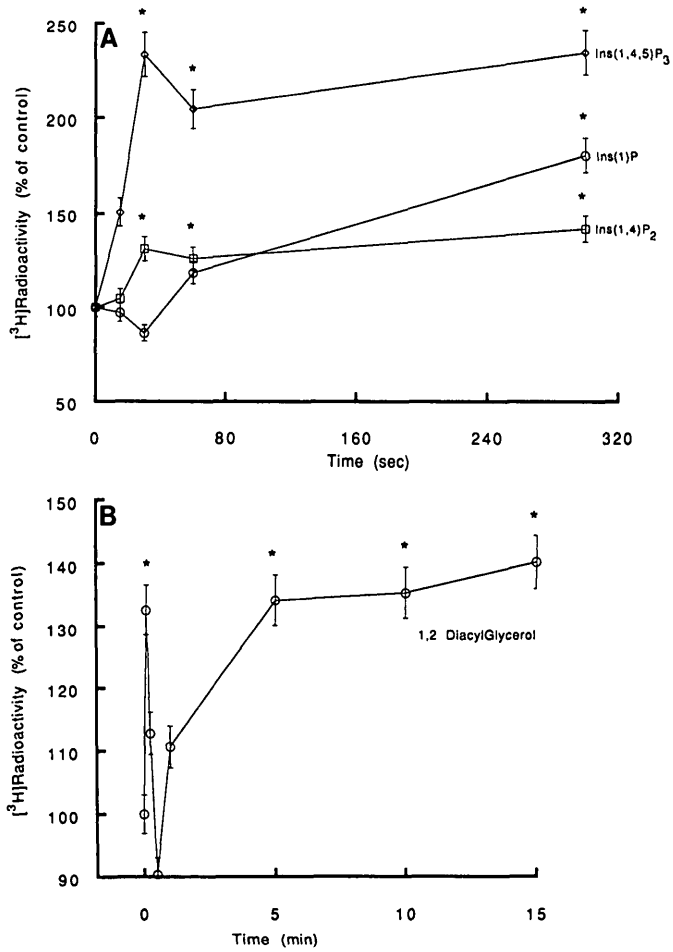

FIG. 10. A, AVP stimulation of inositol phosphates production. A_7r_5 cells preincubated with [^{3}H]myoinositol were stimulated by AVP for 15 sec to 5 min. The different radiolabeled phosphoinositides were separated by Dowex chromatography before measurement of ^{3}H radioactivity (n = 6, *, $P < 0.05$ compared to respective control series). B, AVP stimulation of 1,2 diacylglycerol production. A_7r_5 cells preincubated with [^{3}H]arachidonate were stimulated by AVP for 15 sec to 15 min. The different radiolabeled phospholipids were separated by TLC before measurement of ^{3}H radioactivity (n = 6, *, $P < 0.05$ compared to respective control series).

vs. 6,960 ± 1,253 cpm). Ins[1,4]P_2 increased rapidly and remained at a steady level (+142% at 5 min, 720 ± 84 cpm *vs.* 508 ± 64 cpm). Ins[1,4,5]P_3 increment was rapid and dramatic (+234% at 5 min, 143 ± 22 cpm *vs.* 61 ± 12 cpm). Together, these results confirm that activation of V_1-vascular AVP receptors stimulates a PIP_2-specific phospholipase C, leading to a rapid and sustained production of Ins[1,4,5]P_3.

AVP stimulates the formation of DAG in A_7r_5 cells

AVP stimulates the formation of DAG in A_7r_5 cells in a biphasic manner. A rapid and transient peak was noted within the first min after application of 1 μM AVP and was followed by a secondary and sustained rise reaching a new plateau after 5 min (5504 ± 603 cpm *vs.* 3158 ± 362 cpm, Fig. 10B). This secondary increase in DAG may be due to hydrolysis of alternate phospholipid substrates besides the polyphosphatidylinositols. Since DAG was assessed in A_7r_5 cells labeled to dynamic equilibrium with [^{3}H]arachidonate and then washed free of exogenous label, [^{3}H]DAG most likely reflects phospholipase C or phospholipase D/PA phosphohydrolase activities and not the combined activities of DAG lipase and monoacyl glycerol acyl transferase.

AVP stimulates the hydrolysis of phosphatidylcholine in A_7r_5 cells

To explore alternate phospholipid substrates for phospholipases, we tested the ability of AVP to stimulate phosphatidylcholine hydrolysis via phospholipase D. [^{3}H]Alkyl lyso GPC serves as an exogenous source of substrate for phospholipase D. This lyso phospholipid is relatively permeable across the cell membrane and is rapidly reacylated. The tritium label is in the nonmetabolized sn-1 position of the PtdCho molecule and thus can be used to follow transphosphatidylation. The mecha-

TABLE 3. AVP activation of phospholipase D in A_7r_5 cells

	Phosphatidic acid	Phosphatidylethanol
Control	8,458 ± 908 cpm/well	8,153 ± 1,168 cpm/well
AVP	12,663 ± 1,393 cpm/well[a]	8,837 ± 1,328 cpm/well
Control + ethanol	7,320 ± 879 cpm/well	7,126 ± 922 cpm/well
AVP + ethanol	8,516 ± 854 cpm/well	16,667 ± 1,833 cpm/well[a]

A_7r_5 cells were labeled with [^{3}H]1-O-alkyl lyso glycero-3-phosphocholine for 2 h then stimulated for 15 min by AVP in the presence or absence of ethanol (n = 3 for each series). The chloroform extracts were run on TLC plates after spiking the samples with authentic synthetic PA and PtdEt. The lipids were visualized by UV light after toluidino-2-naphthalene spraying, scraped, and their radioactivity determined in a liquid scintillation counter.

[a] $P < 0.05$ compared to respective control series.

nisms of this reaction involve a phosphatidyl-enzyme intermediate (base exchange) that accepts water as the phosphatidate acceptor. This process can be exploited, as alcohol can substitute for water to form phosphatidylalcohol derivatives (transphosphatidylation). In the presence of exogenous ethanol, activation of phospholipase D will result in the increase of both PA and the product of the transphosphatidylation reaction, *i.e.* PtdEt. Thus, the formation of PtdEt in the presence of exogenous ethanol is conclusive proof of phospholipase D activity, as transphosphatidylation is unique to phospholipase D. Basal phospholipase D activity is minimal in the A_7r_5 cells, at least when the alkyl phosphatidylcholine pool serves as substrate for the reaction, a phenomenon also observed in HL60 granulocytes (24). AVP stimulated a transphosphatidylation reaction in A_7r_5 cells as shown in Table 3. In cells prelabeled with [^{3}H] alkyl lyso GPC in the absence of ethanol, AVP had no effect on the cellular PtdEt levels but increased cellular PA levels by 50%. In the presence of ethanol, the AVP-induced increase in PA was reduced, whereas PtdEt levels doubled. These results suggest that AVP stimulates phospholipase D in A_7r_5 cells.

Discussion

The cardiovascular and trophic effects of AVP are mediated via activation of V_1-vascular receptors which can be investigated by using platelets, hepatocytes, or more appropriately smooth muscle cells. The present study shows that A_7r_5 cells are a convenient cell model to use for the exploration of V_1-vascular AVP receptor signal mechanisms. This immortalized cell line was derived from the thoracic aorta of the rat fetus. It shares many of the characteristics of smooth muscle cells, including the presence of a well developed rough endoplasmic reticulum and dispersed filaments. By using this sturdy and easy to grow cell line, one avoids interanimal variability problems and eliminates the modulating effects of diverse factors (*e.g.* circulating hormone, the sodium content of the diet, gender, thyroid hormones, and steroids) on AVP receptors' characteristics (14, 28). Moreover, the use of an immortalized cell line avoids the problems of receptor loss and decreased responsiveness encountered in primary cell cultures (29).

[^{3}H]AVP specifically binds to a low capacity, high affinity single class of sites on A_7r_5 cells. [^{3}H]AVP specific binding is saturable with time, dependent on the concentration of both the ligand and protein, and reversible. The equilibrium dissociation constant we observed in A_7r_5 cells for [^{3}H]AVP (K_d = 2.11 nM) is in agreement with the dissociation constant values reported in the literature for V_1-vascular AVP receptors of rat mesenteric arteries [K_d = 5.1 nM (30)], rat aorta [K_d = 1.6 nM (31)], rat aortic smooth muscle cells in culture [K_d = 12 nM, (13)], and of the vascular smooth cell line A-10 [K_d = 6 nM (32)]. Recently, Jans *et al.* (33) labeled A_7r_5 cells with the fluorescent AVP analog 1-deamino[8-lysine(N6-tetramethylrhodamylaminothiocarbonyl)]vasopressin and reported lateral mobility and internalization of AVP receptors. Their values for affinity and capacity of the V_1-vascular AVP receptors of A_7r_5 cells are similar to our figures (K_d = 1.83 *vs.* 2.11 nM, B_{max} = 386 *vs.* 306 fmol/mg protein) when using [^{3}H]AVP as a radioligand. Our study shows that the affinity and capacity of the agonist radioligand binding to V_1-vascular AVP receptors of A_7r_5 cells are modulated by the presence of divalent cations and guanine nucleotide analogs (or their substitute aluminum fluoride). This divalent cation dependence of agonist binding is a typical characteristic of V_1-vascular AVP receptors as it is also observed for V_1-vascular AVP receptors of human platelets (3) and hepatocytes (12). Experiments conducted with $MgCl_2$, aluminum fluoride, and the agonist and antagonist radioligands suggest that V_1-vascular AVP receptors are coupled to a guanine nucleotide regulatory protein, following a pattern reported for adenosine and dopamine receptors (34). In our study, we further characterized V_1-vascular AVP receptors of A_7r_5 cells with the V_1 antagonist radioligand [^{3}H] $d(CH_2)_5$Tyr(Me)AVP, which displayed a greater affinity than [^{3}H]AVP for the V_1-vascular AVP receptors of A_7r_5 cells. At variance with agonist binding, the characteristics of antagonist binding are divalent cation independent, hence one may prefer [^{3}H]$d(CH_2)_5$Tyr(Me)AVP when conducting RRAs.

Fura-2 is a convenient and sensitive tool to explore dynamic alterations of $[Ca^{++}]_i$. The baseline $[Ca^{++}]_i$ value noted in our study (136 nM) is close to that observed in other smooth muscle cell lines such as the DDT_1 and A10 cells (140 nM) (21). A rise in $[Ca^{++}]_i$ is an early signal triggered by binding of AVP to V_1-vascular receptors. In A_7r_5 cells, the K_d value (2.11 nM) for [^{3}H]AVP binding and the EC_{50} value (1.87 nM) for AVP-

induced $[Ca^{++}]_i$ increase are similar, therefore confirming the close tie between both events. AVP-induced $[Ca^{++}]_i$ mobilization is blocked by preaddition of the specific V_1-vascular antagonist $d(CH_2)_5Tyr(Me)AVP$, in agreement with the V_1-vascular subtype of AVP receptors involved. The rapid desensitization we observed after the second AVP application was also recently reported by Caramelo *et al.* (35) in vascular smooth muscle cells. These authors found that the homologous AVP desensitization was rapid, dose-dependent, and related to hormone receptor occupancy and protein kinase C activation, but not to receptor internalization.

Our data suggest that the initial spike increase in $[Ca^{++}]_i$ results from both intracellular calcium release from the endoplasmic reticulum and influx of extracellular calcium. The secondary sustained increase in $[Ca^{++}]_i$ is due to influx of extracellular calcium as it is abolished by EDTA and extracellular calcium depletion. The rapid rise of inositol trisphosphate suggests that mobilization of intracellular calcium stores by AVP occurs via receptor-dependent activation of PIP_2-specific phospholipase C. Experiments with tBuBHQ, a relatively selective inhibitor of the endoplasmic reticulum Ca^{++}ATPase, are consistent with release of calcium by AVP from the endoplasmic reticulum pool sensitive to inositol trisphosphate. The initial and rapid production of DAG induced by AVP provides corroborative evidence for a phospholipase C signal transduction pathway which is linked to the activation of protein kinase C. In A_7r_5 cells treated with tBuBHQ and stimulated by AVP, a steady return of $[Ca^{++}]_i$ to basal levels was observed, suggesting that AVP-stimulated $[Ca^{++}]_i$ transients are controlled in part by a hormone-dependent calcium efflux pathway which does not involve reuptake into the endoplasmic reticulum. Indeed, Doyle and Rüegg (36) have shown that AVP increased the efflux of $^{45}Ca^{++}$ from preloaded A_7r_5 cells, and Vigne *et al.* (37) have reported the presence of a Na^+/Ca^{++} antiporter in A_7r_5 cells, which was sensitive to amiloride derivatives but insensitive to blockers of voltage-operated Ca^{++} channels.

The magnitude and duration of the sustained phase of $[Ca^{++}]_i$ increase produced by AVP in A_7r_5 cells is similar to what is observed with other peptides like angiotensin II and norepinephrine. The experiments performed with Mn^{++}, a cation that permeates Ca^{++} selective channels, demonstrate that AVP rapidly triggers Ca^{++} uptake across A_7r_5 cell plasma membranes. Our data indicate that calcium influx induced by AVP is independent of voltage-operated channels as it is unaltered by preaddition of the dihydropyridine antagonist nicardipine. The reduction of AVP-induced $[Ca^{++}]_i$ increase in the presence of extracellular Ca^{++} by indomethacin suggests that phospholipase A_2 and AA metabolites are also instrumental in AVP stimulation of Ca^{++} influx. Measuring AVP-stimulated release of radiolabeled arachidonic acid metabolites by A-10 smooth muscle cells, Welsh *et al.* (38) observed that the activity of phospholipase A_2 appeared to be extracellular Ca^{++}-sensitive. Our data suggest that activation of the arachidonate pathways is involved in the AVP-induced influx of extracellular Ca^{++} in A_7r_5 cells.

The activation of V_1-vascular AVP of A_7r_5 cells stimulates a rapid hydrolysis of PIP_2 in Ins[1,4,5]P_3 and DAG contemporary to the initial $[Ca^{++}]_i$ increase, suggesting coupling to phospholipase C. Second messengers derived from the hydrolysis of PtdCho may augment or sustain this initial event. We have shown that AVP induces a biphasic elevation of DAG in A_7r_5 cells. The sustained accumulation of DAG may reflect phospholipase C hydrolysis of phospholipid substrates besides the polyphosphoinositides. In addition, the sustained DAG production may reflect sequential phospholipase D/PA phosphohydrolase activities. We have demonstrated conclusively an AVP-stimulated phospholipase D activity which uses PtdCho as a substrate. AVP stimulates the accumulation of PtdEt, a transphosphatidylation product of phospholipase D, which has been used in various cell models as a marker of phospholipase D activity. Phospholipase D hydrolyzes phospholipid substrates to yield PA which stimulates $[Ca^{++}]_i$ increase and cell proliferation in other cell systems (23). Furthermore, AVP-stimulated phospholipase D may sustain protein kinase C activation, a modulator of contraction and proliferation, through PA phosphohydrolase-generated DAG formation (16, 39, 40). Thus, we suggest that additional signal transduction pathways which hydrolyze PtdCho via either phospholipase C or D function as important regulators of smooth muscle cell homeostasis.

In conclusion, high affinity V_1-vascular AVP receptors are present at the surface of A_7r_5 cells. Their activation leads to a dramatic rise in intracellular free calcium lasting a few minutes. Contemporary to the Ca^{++} alterations is noted an activation of phospholipases A_2, C, and D, critical events in Ca^{++} homeostasis and cell mitogenesis.

Acknowledgments

We would like to thank Dr. George Dubyak for sharing with us his expertise on calcium signaling in A_7r_5 cells.

References

1. Thibonnier M 1988 Use of vasopressin antagonists in human diseases. Kidney Int 34 [Suppl 26]:S48–S51
2. Thibonnier M, Roberts JM 1985 Characterization of the human platelet vasopressin receptors. J Clin Invest 76:1857–1864
3. Thibonnier M, Hinko A, Pearlmutter AF 1987 The human platelet vasopressin receptor and its intracellular messengers: key role of divalent cations. J Cardiovasc Pharmacol 10:24–29
4. Thibonnier M 1987 Solubilization of human platelet vasopressin

receptors. Life Sci 40:439–445
5. Thibonnier M 1987 Purification of the human platelet vasopressin receptor. Identification by direct UV photoaffinity labeling. J Biol Chem 262:10960–10964
6. Thibonnier M, Chehade N, Hinko A 1990 A V_1-vascular vasopressin antagonist suitable for radioiodination and photoaffinity labeling. Am J Hypertension 3:471–475
7. Thibonnier M 1990 Vasopressin agonists and antagonists. Horm Res 34:124–128
8. Thibonnier M, Bayer AL, Simonson ML, Snajdar RM 1990 Reconstitution of solubilized V_1 vasopressin receptors of human platelets. Am J Physiol 259:E751–E756
9. Siess W, Stifel M, Binder H, Weber P 1986 Activation of V_1-receptors by vasopressin stimulates inositol phospholipid hydrolysis and arachidonate metabolism in human platelets. Biochem J 233:83–91
10. Pletscher A, Erne P, Burgisser E, Ferracin P 1985 Activation of human blood platelets by arginine-vasopressin: role of bivalent cations. Mol Pharmacol 28:508–514
11. Vittet D, Rondot A, Cantau A, Launay JM, Chevillard C 1986 Nature and properties of human platelet vasopressin receptors. Biochem J 233:631–636
12. Gopalakrishnan V, McNeill JR, Sulakhe PV, Triggle CR 1988 Hepatic vasopressin receptor: differential effects of divalent cations, guanine nucleotides, and *N*-ethylmaleimide on agonist and antagonist interactions with the V_1 subtype receptor. Endocrinology 123:922–931
13. Penit J, Faure M, Jard S 1983 Vasopressin and angiotensin II receptors in rat aorta smooth muscle cells in culture. Am J Physiol 244:E72–E82
14. St-Louis J, Schiffrin EL 1984 Biological actions and binding sites for vasopressin on the mesenteric artery from normal and sodium-depleted rats. Life Sci 35:1489–1495
15. Exton JH 1990 Signaling through phosphatidylcholine breakdown. J Biol Chem 265:1–8
16. Billah MM, Arthes JC 1990 The regulation and cellular function of phosphatidylcholine hydrolysis. Biochem J 269:281–291
17. Kimes BW, Brandt BL 1976 Characterization of two putative smooth muscle cell lines from rat thoracic aorta. Exp Cell Res 98:349–366
18. Doyle VM, Ruegg UT 1985 Vasopressin induced production of inositol trisphosphate and calcium efflux in a smooth muscle cell line. Biochem Biophys Res Commun 131:469–476
19. Van Renterghem C, Romey G, Lazdunski M 1988 Vasopressin modulates the spontaneous electrical activity in aortic cells (line A_7r_5) by acting on three different types of ionic channels. Proc Natl Acad Sci USA 85:9365–9369
20. Cheng Y, Prusoff WH 1973 Relationship between the inhibition constant (K_i) and the concentration of inhibitor which causes 50 percent inhibition (IC_{50}) of an enzymatic reaction. Biochem Pharmacol 22:3099–3108
21. Reynolds ER, Dubyak GR 1986 Agonist-induced calcium transients in cultured smooth muscle cells: measurements with fura-2 loaded monolayers. Biochem Biophys Res Commun 136:927–934
22. Mene P, Dubyak GR, Abboud HE, Scarpa A, Dunn MJ 1988 Phospholipase C activation by prostaglandins and thromboxane A_2 in cultured mesangial cells. Am J Physiol 255:F1059–F1069
23. Kester M, Simonson MS, Mene P, Sedor JR 1989 Interleukin-1 generates transmembrane signals from phospholipids through novel pathways in cultured rat mesangial cells. J Clin Invest 83:718–723
24. Pai SK, Siegel MI, Egan RW, Billah MM 1988 Activation of phospholipase D by chemoattractant peptide in HL60 cells. Biochem Biophys Res Commun 150:355–364
25. Holford NHG, Sheiner LB 1981 Understanding the dose-effect relationship: clinical application of pharmacokinetic-pharmacodynamic models. Clin Pharmacokinet 6:429–453
26. Kass GE, Duddy BK, Moore GA, Orrensus S 1989 2,5-Di-(terbutyl)-1,4-benzohydroquinone rapidly elevates cytosolic Ca^{++} concentration by mobilizing the inositol 1,4,5-triphosphate-sensitive Ca^{++} pool. J Biol Chem 264:15192–15198
27. Simonson MS, Dunn MJ 1991 Ca^{++} signaling by distinct endothelin peptides in glomerular mesangial cells. Exp Cell Res 192:148–156
28. St-Louis J, Parent A, Lariviere R, Schiffrin EL 1986 Vasopressin responses and receptors in the mesenteric vasculature of estrogen-treated rats. Am J Physiol 251:H885–H889
29. Bouscarel B, Augert G, Taylor SJ, Exton JH 1990 Alterations in vasopressin and angiotensin II receptors and responses during culture of rat liver cells. Biochim Biophys Acta 1055:265–272
30. Schiffrin EL, Genest J 1983 [^{3}H]Vasopressin binding to the rat mesenteric artery. Endocrinology 113:409–411
31. Pearlmutter AF, Szkrybalo M, Pettibone G 1985 Specific arginine vasopressin binding in particulate membrane from rat aorta. Peptides 6:427–431
32. Stassen FL, Heckman G, Schmidt D, Aiyar N, Nambi P, Crooke ST 1987 Identification and characterization of vascular (V_1) vasopressin receptors of an established smooth muscle cell line. Mol Pharmacol 31:259–266
33. Jans DA, Peters R, Fahrenholz F 1990 Lateral mobility of the phospholipase C-activating vasopressin V_1-type receptor in A_7r_5 smooth muscle cells: a comparison with the adenylate cyclase-coupled V_2-receptor. EMBO J 9:2693–2699
34. Goodman RR, Cooper MJ, Snyder SH 1982 Guanine nucleotide and cation regulation of the binding of [^{3}H]cyclohexyladenosine and [^{3}H]diethylphenylxanthine to adenosine A_1 receptors in brain membranes. Mol Pharmacol 21:329–335
35. Caramelo C, Tsai P, Okada K, Briner VA, Schrier RW 1991 Mechanisms of rapid desensitization to arginine vasopressin in vascular smooth muscle cells. Am J Physiol 260:F46–F52
36. Doyle VM, Rüegg UT 1985 Vasopressin induced production of inositol trisphosphate and calcium efflux in a smooth muscle cell line. Biochem Biophys Res Commun 131:469–476
37. Vigne P, Breittmayer JP, Duval D, Freslin C, Lazdunski M 1988 The Na^+/Ca^{++} antiporter in aortic smooth muscle cells. J Biol Chem 263:8078–8083
38. Welsh CJ, Schmeichel K, Cao HT, Chabbott H 1990 Vasopressin stimulates phospholipase D activity against phosphatidylcholine in vascular smooth muscle cells. Lipids 25:675–684
39. Martin TW 1988 Formation of DAG by a phospholipase D-phosphatidate phosphatase pathway specific for phosphatidylcholine in endothelial cells. Biochim Biophys Acta 962:282–296
40. Qian Z, Drewes LR 1990 A novel mechanism for acetylcholine to generate diacylglycerol in brain. J Biol Chem 265:3607–3610
41. Mannig M, Sawyer WH 1989 Discovery, development, and some uses of vasopressin and oxytocin antagonists. J Lab Clin Med 114:617–632